Single-Particle Spectroscopy

DOI: 10.1002/ange.200700033

Spectroscopy and High-Resolution Microscopy of Single Nanocrystals by a Focused Ion Beam Registration Method**

*Carolina Novo, Alison M. Funston, Isabel Pastoriza-Santos, Luis M. Liz-Marzán, and Paul Mulvaney**

The plasmon resonance in small metal particles and structures is extremely sensitive to both the size and the shape of the particle.[1] This feature enables materials to be developed with tunable optical resonances throughout the visible and near-infrared spectral region through changes to the particle morphology. However, chemical synthesis invariably yields a range of particle sizes and frequently different shapes. Thus, the extinction spectra or scattered-light spectra obtained in these cases are statistical averages over all particle sizes and shapes present within the ensemble. This has rendered the determination of the size and shape dependence of surface-plasmon modes a difficult problem.

Recently, new techniques have been developed to allow the study of the optical properties of individual particles: for example, dark-field microscopy (DFM),[2–4] total internal reflection microscopy,[5] and near-field scanning optical microscopy (NSOM).[6] However, using these techniques alone, one cannot determine the exact size and shape of the particle whose optical properties have been measured. Thus, although the scattering spectrum of a single metal particle may be determined, comparison of these results with theory remains a difficult task, since the specific size and shape remains unknown. The combination of single-particle spectroscopy with electron microscopy imaging would allow precise correlation of the size and shape of the nanoparticle with the measured surface-plasmon spectrum. Although results in this direction have been reported,[7–14] most methods used were either very time consuming, or not completely reliable. Early approaches to this problem included the use of a surreptitiously positioned mark, scratch, or piece of dirt as a location marker for the mapping of single molecules[7] or by pattern matching.[8–12] More recently, a reliable method to correlate imaging with nonlinear (second-harmonic) optical measurements of individual particles has been reported. This method employs Si_3N_4 windows on Si wafers marked by lithographic methods with chromium. Imaging was carried out by using TEM.[13–14] This method, although effective for second-harmonic optical measurements, does not allow the correlation of particle size and shape with plasmon excitation because of the small size of the Si_3N_4 windows, the edges of which are efficient light scatterers, and the nature of the light-scattering experiments used to determine the extinction.

Herein, we report a method that can be routinely used to reliably coordinate high-resolution electron microscopy imaging and optical characterization. The procedure makes use of a focused ion beam (FIB) to create micrometer-scale "landmarks" in a conducting glass substrate that can be used to register and locate the same nanocrystals repeatedly.

Samples were prepared by spin-coating the nanoparticle solution on top of ITO-covered glass slides (ITO = indium tin oxide) onto which a thin layer of poly(methyl methacrylate) (PMMA) had been spin-coated. For the measurements outlined below, the nanoparticle solution was synthesized by using the seed-mediated method developed by Sánchez-Iglesias et al.[15] The sample was marked by using the FIB of an xT Nova NanoLab instrument to allow easy identification of an area of the glass slide containing nanoparticles. The corners of a box (50 μm × 50 μm in size) were milled into the slide as shown in Figure 1. Each box contained a unique mark pattern to allow differentiation of the boxes (see, for example, lower left corner of box in Figure 1).

The scattering spectra of individual particles within the box and adjacent areas were recorded with a Nikon Eclipse TE-2000 microscope coupled to a Nikon dark-field condenser (Dry, 0.95–0.80 NA). The scattered light was collected with a Nikon Plan Fluor ELWD 40 × /0.60 NA objective and focused onto the entrance port of a MicroSpec 2150i imaging spectrometer coupled with a TE-cooled CCD camera

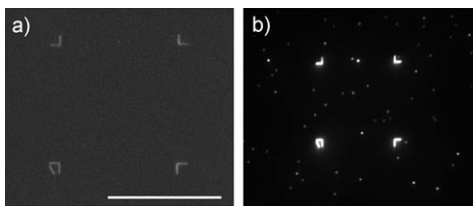

Figure 1. a) SEM and b) DFM images of a box milled onto an ITO-covered glass slide by using an FIB/scanning electron microscope. Scale bar = 50 μm.

[*] C. Novo, Dr. A. M. Funston, Prof. P. Mulvaney
School of Chemistry
The University of Melbourne
Victoria, 3010 (Australia)
Fax: (+61) 3-9347-5180
E-mail: mulvaney@unimelb.edu.au
Homepage: http://www.nanoparticle.com
Dr. I. Pastoriza-Santos, Prof. L. M. Liz-Marzán
Departamento de Química Física and
Unidad Asociada CSIC
Universidade de Vigo
Campus Universitario, 36310, Vigo (Spain)

[**] C.N., A.M.F., and P.M. were supported by the Australian Research Council (DP Grant 0558608 and FF0561486). I.P.-S. and L.M.L.-M. were supported by the Spanish Ministerio de Educación y Ciencia (Grants MAT2004-02991 and NAN2004-09133). C.N. acknowledges the University of Melbourne for the MIRS and MIFRS scholarships. I.P.-S. acknowledges the Xunta de Galicia for an Isidro Parga Pondal fellowship.

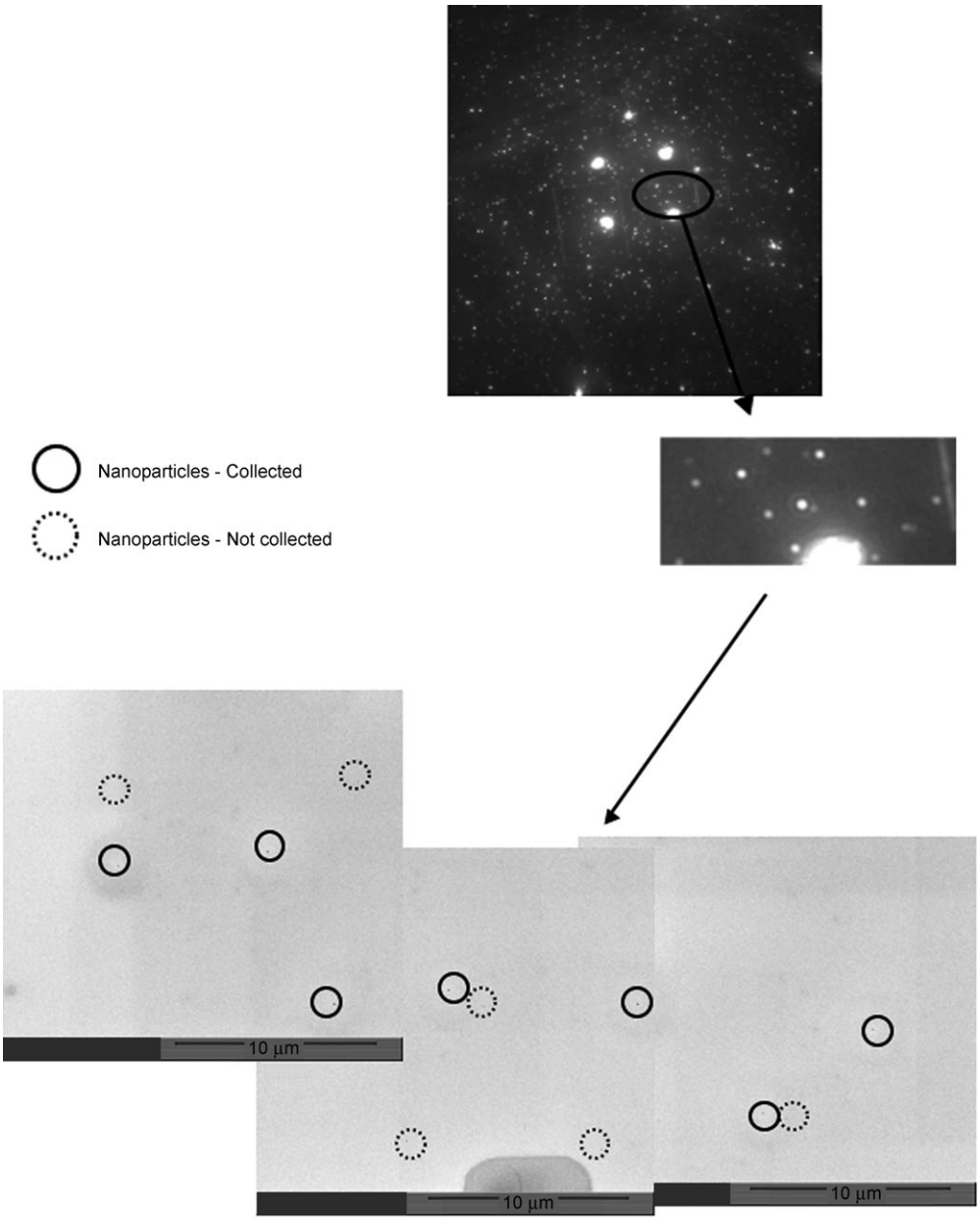

Figure 2. Mapping process: The sample (box area) is imaged by dark-field microscopy (top), and then each individual particle is imaged in a scanning electron microscope (bottom). The matching patterns (dark-field and SEM) are proof that the spectrum and image of a same particle are being collected. The particles closest to the box are not readily apparent in the dark-field image because of the scattering of the milled box corners. The SEM image has been color-inverted to improve clarity.

(PIXIS 1024 ACTON Princeton Instruments). The light scattered by each particle was observed through our CCD as a light dot of approximately 10×10 pixels. Along with the spectra, images of the areas within and around the boxes were collected and mapped to allow correlation of particle position with spectra. The mapping process is depicted in Figure 2. In this figure, the dark-field image of the whole box is apparent, and the expansion shows the area imaged later in the scanning electron microscope. The SEM images shown in Figure 2 were color-inverted to facilitate viewing of the nanoparticles, which appear as small black dots. Images of the particles corresponding to each spectrum (as determined from the mapping) were obtained by using the SEM functionality of the xT Nova NanoLab. Modern SEM resolution is comparable to normal-resolution TEM and therefore allows precise particle characterization.

The use of the boxes as orienting markers thus allows the spectrum of a gold nanoparticle with known shape and size to be measured, that is, one specific particle can be imaged and its plasmon spectrum collected. The technique does not rely on the serendipitous location of an easily identifiable mark, pattern, or constellation of particles within the sample.[16] Importantly, the depth of the FIB structure must be tuned so as not to introduce excess light scattering into the dark-field microscope. A depth of 0.5–1.0 µm is sufficient for routine recognition in the optical microscope and by SEM without increasing the background scatter during DFM. This technique increases the reliability of the particle–spectrum correlation and allows efficient collection of a large number of uniquely identified nanoparticle plasmon spectra.

Figure 3 shows scattering spectra and SEM images of gold nanoparticles of known size and shape. All particles were part of the same colloid preparation, which contained 58% nanodecahedrons and 42% nanotriangles, along with a small number of nanohexagons and nanooctahedrons. As expected, nanoparticles of the same size but different shape have bands located at different positions. The spectra show that the larger the particle, the more red-shifted the plasmon band (Table 1), which is consistent with ensemble and single-particle measurements of colloid preparations with different average particle sizes. An unexpected outcome of this investigation is that gold nanotriangles on average scatter light far more efficiently than nanodecahe-

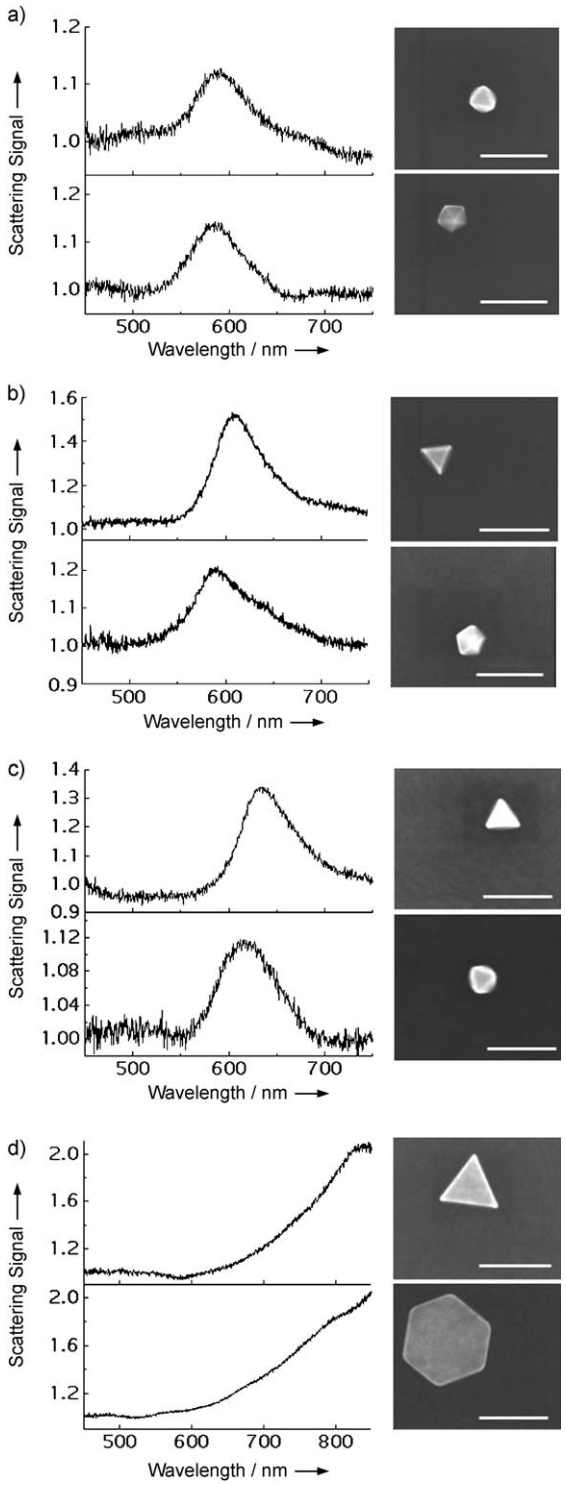

Figure 3. SEM images and corresponding scattering spectra of gold nanoparticles. a) Nanooctahedron and nanodecahedron, both with side of 81.3 nm. b) Nanotriangle and nanodecahedron, 90 and 90.3 nm, respectively (side). c) Nanotriangle and nanooctahedron, 100 nm and 97.5 nm, respectively (side). d) Nanotriangle and nanohexagon, 167.8 nm (side) and 264.5 nm (diameter across from point to point), respectively. Scale bars = 200 nm.

drons of similar size. As a result, measurements carried out without knowledge of the shape of the nanoparticle may be easily biased towards the spectra of nanotriangles, despite the fact that there is a much larger proportion of nanodecahedrons present in the sample, which again confirms the importance of being able to identify the size and shape of the individual particle. Similarly, larger particles scatter light more efficiently, and therefore the collection of single-particle spectra would also be biased towards larger particles, which would make average values meaningless. Also present in the sample were a number of dimers and aggregates. The correlated method allows these to be distinguished from single particles, which was previously very difficult, and their interactions and dependence on particle position investigated. These findings highlight the importance of imaging correlated with plasmon spectroscopy.

Table 1: Absorption maxima of gold nanoparticles of specific sizes and shapes.

Particle shape	Size [nm][a]	λ_{max} [nm]
nanotriangle	90	610
	100	635
	167.8	839
nanodecahedron	81.3	584
	90.3	591
nanooctahedron	81.3	590
	97.5	617
nanohexagon	264.5	>850

[a] Length of side, except for nanohexagon, for which diameter from point to point is given.

This new method for simultaneous analysis of particle size, shape, and scattering spectrum is a step forward in the study of optical properties of single nanoparticles. It allows concurrent dark-field imaging and electron microscopy imaging of the same micrometer-scale surface regions. It avoids the inhomogeneity effects inherent in any single-particle study carried out without identification of the size and shape of each particle investigated as well as any systematic bias towards a particular particle size and shape. It can be used for luminescent semiconductor particles as well as metallic particles. Importantly, it will in the future allow detailed tests of theoretical models describing the optical properties of nanoparticles. A detailed discrete dipole approximation (DDA) analysis of single gold and silver nanoparticles will be presented elsewhere.

Received: January 3, 2007
Revised: February 19, 2007
Published online: March 30, 2007

Keywords: electron microscopy · focused ion beam · morphology · single-particle studies · surface plasmon resonance

[1] L. M. Liz-Marzán, *Langmuir* **2006**, *22*, 32.
[2] C. Novo, D. Gomez, J. Perez-Juste, Z. Y. Zhang, H. Petrova, M. Reismann, P. Mulvaney, G. V. Hartland, *Phys. Chem. Chem. Phys.* **2006**, *8*, 3540.
[3] A. Arbouet, D. Christofilos, N. Del Fatti, F. Vallee, J. R. Huntzinger, L. Arnaud, P. Billaud, M. Broyer, *Phys. Rev. Lett.* **2004**, *93*.

[4] M. Hu, H. Petrova, A. R. Sekkinen, J. Y. Chen, J. M. McLellan, Z. Y. Li, M. Marquez, X. D. Li, Y. N. Xia, G. V. Hartland, *J. Phys. Chem. B* **2006**, *110*, 19923.
[5] a) C. Sönnichsen, S. Geier, N. E. Hecker, G. von Plessen, J. Feldmann, H. Ditlbacher, B. Lamprecht, J. R. Krenn, F. R. Aussenegg, V. Z. H. Chan, J. P. Spatz, M. Moller, *Appl. Phys. Lett.* **2000**, *77*, 2949; b) C. Sönnichsen, T. Franzl, T. Wilk, G. von Plessen, J. Feldman, O. Wilson, P. Mulvaney, *Phys. Rev. Lett.* **2002**, *88*, 077402.
[6] H. Okamoto, K. Imura, *J. Mater. Chem.* **2006**, *16*, 3920.
[7] T. H. Lee, J. I. Gonzalez, J. Zheng, R. M. Dickson, *Acc. Chem. Res.* **2005**, *38*, 534.
[8] J. J. Mock, M. Barbic, D. R. Smith, D. A. Schultz, S. Schultz, *J. Chem. Phys.* **2002**, *116*, 6755.
[9] J. J. Mock, S. J. Oldenburg, D. R. Smith, D. A. Schultz, S. Schultz, *Nano Lett.* **2002**, *2*, 465.
[10] C. L. Nehl, N. K. Grady, G. P. Goodrich, F. Tam, N. J. Halas, J. H. Hafner, *Nano Lett.* **2004**, *4*, 2355.
[11] C. L. Nehl, H. W. Liao, J. H. Hafner, *Nano Lett.* **2006**, *6*, 683.
[12] H. Tamaru, H. Kuwata, H. T. Miyazaki, K. Miyano, *Appl. Phys. Lett.* **2002**, *80*, 1826.
[13] R. C. Jin, J. E. Jureller, H. Y. Kim, N. F. Scherer, *J. Am. Chem. Soc.* **2005**, *127*, 12482.
[14] R. C. Jin, J. E. Jureller, N. F. Scherer, *Appl. Phys. Lett.* **2006**, *88*, 263111.
[15] A. Sánchez-Iglesias, I. Pastoriza-Santos, J. Pérez-Juste, B. Rodríguez-González, F. J. García de Abajo, L. M. Liz-Marzán, *Adv. Mater.* **2006**, *18*, 2529.
[16] P. Mulvaney, M. Giersig, *Faraday Trans.* **1996**, *92*, 3137.

